BABAR-CONF-01/28
SLAC-PUB-8982
September, 2001
hep-ex/0109009

Study of $B \to D^{(*)}\overline{D}^{(*)}$ decays with the *BABAR* detector

The *BABAR* Collaboration

Abstract

Decays of the type $B \to D^{(*)}\overline{D}^{(*)}$ can be used to provide a measurement of the parameter $\sin 2\beta$ of the Unitarity Triangle that is complementary to that derived from the mode $B^0 \to J/\psi K^0_S$. Here we report a measurement of the branching fraction and a study of the *CP* parity content for the decay $B^0 \to D^{*+}D^{*-}$ with the *BABAR* detector. With data corresponding to an integrated luminosity of $20.7\,\mathrm{fb}^{-1}$ collected at the $\Upsilon(4S)$ resonance during 1999-2000, we determine the branching fraction to be $\mathcal{B}(B^0 \to D^{*+}D^{*-}) = (8.0 \pm 1.6(stat) \pm 1.2(syst)) \times 10^{-4}$. The measured fraction of the component with odd *CP* parity is $0.22 \pm 0.18(stat) \pm 0.03(syst)$. Observation of a significant number of candidates in the decay modes $B^0 \to D^{*+}D^{-}$ and $B^+ \to D^{*+}D^{*0}$ is reported. All results presented in this note are preliminary.

Submitted to the 9^{th} International Symposium On Heavy Flavor Physics,
9/10—9/13/2001, Pasadena, CA, USA

Stanford Linear Accelerator Center, Stanford University, Stanford, CA 94309

Work supported in part by Department of Energy contract DE-AC03-76SF00515.

The *BABAR* Collaboration,

B. Aubert, D. Boutigny, J.-M. Gaillard, A. Hicheur, Y. Karyotakis, J. P. Lees, P. Robbe, V. Tisserand

Laboratoire de Physique des Particules, F-74941 Annecy-le-Vieux, France

A. Palano, A. Pompili

Università di Bari, Dipartimento di Fisica and INFN, I-70126 Bari, Italy

G. P. Chen, J. C. Chen, N. D. Qi, G. Rong, P. Wang, Y. S. Zhu

Institute of High Energy Physics, Beijing 100039, China

G. Eigen, B. Stugu

University of Bergen, Inst. of Physics, N-5007 Bergen, Norway

G. S. Abrams, A. W. Borgland, A. B. Breon, D. N. Brown, J. Button-Shafer, R. N. Cahn, A. R. Clark, M. S. Gill, A. V. Gritsan, Y. Groysman, R. G. Jacobsen, R. W. Kadel, J. Kadyk, L. T. Kerth, Yu. G. Kolomensky, J. F. Kral, C. LeClerc, M. E. Levi, G. Lynch, P. J. Oddone, A. Perazzo, M. Pripstein, N. A. Roe, A. Romosan, M. T. Ronan, V. G. Shelkov, A. V. Telnov, W. A. Wenzel

Lawrence Berkeley National Laboratory and University of California, Berkeley, CA 94720, USA

P. G. Bright-Thomas, T. J. Harrison, C. M. Hawkes, D. J. Knowles, S. W. O'Neale, R. C. Penny, A. T. Watson, N. K. Watson

University of Birmingham, Birmingham, B15 2TT, United Kingdom

T. Deppermann, K. Goetzen, H. Koch, M. Kunze, B. Lewandowski, K. Peters, H. Schmuecker, M. Steinke

Ruhr Universität Bochum, Institut für Experimentalphysik 1, D-44780 Bochum, Germany

J. C. Andress, N. R. Barlow, W. Bhimji, N. Chevalier, P. J. Clark, W. N. Cottingham, N. De Groot,[1] N. Dyce, B. Foster, J. D. McFall, D. Wallom, F. F. Wilson

University of Bristol, Bristol BS8 1TL, United Kingdom

K. Abe, C. Hearty, T. S. Mattison, J. A. McKenna, D. Thiessen

University of British Columbia, Vancouver, BC, Canada V6T 1Z1

S. Jolly, A. K. McKemey, J. Tinslay

Brunel University, Uxbridge, Middlesex UB8 3PH, United Kingdom

V. E. Blinov, A. D. Bukin, D. A. Bukin, A. R. Buzykaev, V. B. Golubev, V. N. Ivanchenko, A. A. Korol, E. A. Kravchenko, A. P. Onuchin, A. A. Salnikov, S. I. Serednyakov, Yu. I. Skovpen, V. I. Telnov, A. N. Yushkov

Budker Institute of Nuclear Physics, Novosibirsk 630090, Russia

D. Best, A. J. Lankford, M. Mandelkern, S. McMahon, D. P. Stoker

University of California at Irvine, Irvine, CA 92697, USA

A. Ahsan, K. Arisaka, C. Buchanan, S. Chun

University of California at Los Angeles, Los Angeles, CA 90024, USA

[1] Also with Rutherford Appleton Laboratory, Chilton, Didcot, Oxon, OX11 0QX, United Kingdom

J. G. Branson, D. B. MacFarlane, S. Prell, Sh. Rahatlou, G. Raven, V. Sharma

University of California at San Diego, La Jolla, CA 92093, USA

C. Campagnari, B. Dahmes, P. A. Hart, N. Kuznetsova, S. L. Levy, O. Long, A. Lu, J. D. Richman, W. Verkerke, M. Witherell, S. Yellin

University of California at Santa Barbara, Santa Barbara, CA 93106, USA

J. Beringer, D. E. Dorfan, A. M. Eisner, A. A. Grillo, M. Grothe, C. A. Heusch, R. P. Johnson, W. S. Lockman, T. Pulliam, H. Sadrozinski, T. Schalk, R. E. Schmitz, B. A. Schumm, A. Seiden, M. Turri, W. Walkowiak, D. C. Williams, M. G. Wilson

University of California at Santa Cruz, Institute for Particle Physics, Santa Cruz, CA 95064, USA

E. Chen, G. P. Dubois-Felsmann, A. Dvoretskii, D. G. Hitlin, S. Metzler, J. Oyang, F. C. Porter, A. Ryd, A. Samuel, M. Weaver, S. Yang, R. Y. Zhu

California Institute of Technology, Pasadena, CA 91125, USA

S. Devmal, T. L. Geld, S. Jayatilleke, G. Mancinelli, B. T. Meadows, M. D. Sokoloff

University of Cincinnati, Cincinnati, OH 45221, USA

T. Barillari, P. Bloom, M. O. Dima, S. Fahey, W. T. Ford, D. R. Johnson, U. Nauenberg, A. Olivas, P. Rankin, J. Roy, S. Sen, J. G. Smith, W. C. van Hoek, D. L. Wagner

University of Colorado, Boulder, CO 80309, USA

J. Blouw, J. L. Harton, M. Krishnamurthy, A. Soffer, W. H. Toki, R. J. Wilson, J. Zhang

Colorado State University, Fort Collins, CO 80523, USA

R. Aleksan, G. De Domenico, A. de Lesquen, S. Emery, A. Gaidot, S. F. Ganzhur, P.-F. Giraud, G. Hamel de Monchenault, W. Kozanecki, M. Langer, G. W. London, B. Mayer, B. Serfass, G. Vasseur, Ch. Yèche, M. Zito

DAPNIA, Commissariat à l'Energie Atomique/Saclay, F-91191 Gif-sur-Yvette, France

T. Brandt, J. Brose, T. Colberg, M. Dickopp, R. S. Dubitzky, A. Hauke, E. Maly, R. Müller-Pfefferkorn, S. Otto, K. R. Schubert, R. Schwierz, B. Spaan, L. Wilden

Technische Universität Dresden, Institut für Kern- und Teilchenphysik, D-01062, Dresden, Germany

D. Bernard, G. R. Bonneaud, F. Brochard, J. Cohen-Tanugi, S. Ferrag, E. Roussot, S. T'Jampens, Ch. Thiebaux, G. Vasileiadis, M. Verderi

Ecole Polytechnique, F-91128 Palaiseau, France

A. Anjomshoaa, R. Bernet, A. Khan, D. Lavin, F. Muheim, S. Playfer, J. E. Swain

University of Edinburgh, Edinburgh EH9 3JZ, United Kingdom

M. Falbo

Elon University, Elon University, NC 27244-2010, USA

C. Borean, C. Bozzi, S. Dittongo, L. Piemontese

Università di Ferrara, Dipartimento di Fisica and INFN, I-44100 Ferrara, Italy

E. Treadwell

Florida A&M University, Tallahassee, FL 32307, USA

F. Anulli,[2] R. Baldini-Ferroli, A. Calcaterra, R. de Sangro, D. Falciai, G. Finocchiaro, P. Patteri, I. M. Peruzzi,[3] M. Piccolo, Y. Xie, A. Zallo

Laboratori Nazionali di Frascati dell'INFN, I-00044 Frascati, Italy

S. Bagnasco, A. Buzzo, R. Contri, G. Crosetti, M. Lo Vetere, M. Macri, M. R. Monge, S. Passaggio, F. C. Pastore, C. Patrignani, M. G. Pia, E. Robutti, A. Santroni, S. Tosi

Università di Genova, Dipartimento di Fisica and INFN, I-16146 Genova, Italy

M. Morii

Harvard University, Cambridge, MA 02138, USA

R. Bartoldus, R. Hamilton, U. Mallik

University of Iowa, Iowa City, IA 52242, USA

J. Cochran, H. B. Crawley, P.-A. Fischer, J. Lamsa, W. T. Meyer, E. I. Rosenberg

Iowa State University, Ames, IA 50011-3160, USA

G. Grosdidier, C. Hast, A. Höcker, H. M. Lacker, S. Laplace, V. Lepeltier, A. M. Lutz, S. Plaszczynski, M. H. Schune, S. Trincaz-Duvoid, G. Wormser

Laboratoire de l'Accélérateur Linéaire, F-91898 Orsay, France

R. M. Bionta, V. Brigljević , D. J. Lange, M. Mugge, K. van Bibber, D. M. Wright

Lawrence Livermore National Laboratory, Livermore, CA 94550, USA

M. Carroll, J. R. Fry, E. Gabathuler, R. Gamet, M. George, M. Kay, D. J. Payne, R. J. Sloane, C. Touramanis

University of Liverpool, Liverpool L69 3BX, United Kingdom

M. L. Aspinwall, D. A. Bowerman, P. D. Dauncey, U. Egede, I. Eschrich, N. J. W. Gunawardane, J. A. Nash, P. Sanders, D. Smith

University of London, Imperial College, London, SW7 2BW, United Kingdom

D. E. Azzopardi, J. J. Back, P. Dixon, P. F. Harrison, R. J. L. Potter, H. W. Shorthouse, P. Strother, P. B. Vidal, M. I. Williams

Queen Mary, University of London, E1 4NS, United Kingdom

G. Cowan, S. George, M. G. Green, A. Kurup, C. E. Marker, P. McGrath, T. R. McMahon, S. Ricciardi, F. Salvatore, I. Scott, G. Vaitsas

University of London, Royal Holloway and Bedford New College, Egham, Surrey TW20 0EX, United Kingdom

D. Brown, C. L. Davis

University of Louisville, Louisville, KY 40292, USA

J. Allison, R. J. Barlow, J. T. Boyd, A. C. Forti, J. Fullwood, F. Jackson, G. D. Lafferty, N. Savvas, E. T. Simopoulos, J. H. Weatherall

University of Manchester, Manchester M13 9PL, United Kingdom

[2] Also with Università di Perugia, I-06100 Perugia, Italy
[3] Also with Università di Perugia, I-06100 Perugia, Italy

A. Farbin, A. Jawahery, V. Lillard, J. Olsen, D. A. Roberts, J. R. Schieck
University of Maryland, College Park, MD 20742, USA

G. Blaylock, C. Dallapiccola, K. T. Flood, S. S. Hertzbach, R. Kofler, V. G. Koptchev, T. B. Moore, H. Staengle, S. Willocq
University of Massachusetts, Amherst, MA 01003, USA

B. Brau, R. Cowan, G. Sciolla, F. Taylor, R. K. Yamamoto
Massachusetts Institute of Technology, Laboratory for Nuclear Science, Cambridge, MA 02139, USA

M. Milek, P. M. Patel
McGill University, Montréal, QC, Canada H3A 2T8

F. Palombo
Università di Milano, Dipartimento di Fisica and INFN, I-20133 Milano, Italy

J. M. Bauer, L. Cremaldi, V. Eschenburg, R. Kroeger, J. Reidy, D. A. Sanders, D. J. Summers
University of Mississippi, University, MS 38677, USA

J. P. Martin, J. Y. Nief, R. Seitz, P. Taras, V. Zacek
Université de Montréal, Laboratoire René J. A. Lévesque, Montréal, QC, Canada H3C 3J7

H. Nicholson, C. S. Sutton
Mount Holyoke College, South Hadley, MA 01075, USA

N. Cavallo,[4] G. De Nardo, F. Fabozzi, C. Gatto, L. Lista, P. Paolucci, D. Piccolo, C. Sciacca
Università di Napoli Federico II, Dipartimento di Scienze Fisiche and INFN, I-80126, Napoli, Italy

J. M. LoSecco
University of Notre Dame, Notre Dame, IN 46556, USA

J. R. G. Alsmiller, T. A. Gabriel, T. Handler
Oak Ridge National Laboratory, Oak Ridge, TN 37831, USA

J. Brau, R. Frey, M. Iwasaki, N. B. Sinev, D. Strom
University of Oregon, Eugene, OR 97403, USA

F. Colecchia, F. Dal Corso, A. Dorigo, F. Galeazzi, M. Margoni, G. Michelon, M. Morandin, M. Posocco, M. Rotondo, F. Simonetto, R. Stroili, E. Torassa, C. Voci
Università di Padova, Dipartimento di Fisica and INFN, I-35131 Padova, Italy

M. Benayoun, H. Briand, J. Chauveau, P. David, Ch. de la Vaissière, L. Del Buono, O. Hamon, F. Le Diberder, Ph. Leruste, J. OCARIZ, L. Roos, J. Stark, S. Versillé
Universités Paris VI et VII, Lab de Physique Nucléaire H. E., F-75252 Paris, France

P. F. Manfredi, V. Re, V. Speziali
Università di Pavia, Dipartimento di Elettronica and INFN, I-27100 Pavia, Italy

[4] Also with Università della Basilicata, I-85100 Potenza, Italy

E. D. Frank, L. Gladney, Q. H. Guo, J. Panetta

University of Pennsylvania, Philadelphia, PA 19104, USA

C. Angelini, G. Batignani, S. Bettarini, M. Bondioli, M. Carpinelli, F. Forti, M. A. Giorgi, A. Lusiani, F. Martinez-Vidal, M. Morganti, N. Neri, E. Paoloni, M. Rama, G. Rizzo, F. Sandrelli, G. Simi, G. Triggiani, J. Walsh

Università di Pisa, Scuola Normale Superiore and INFN, I-56010 Pisa, Italy

M. Haire, D. Judd, K. Paick, L. Turnbull, D. E. Wagoner

Prairie View A&M University, Prairie View, TX 77446, USA

J. Albert, P. Elmer, C. Lu, K. T. McDonald, V. Miftakov, S. F. Schaffner, A. J. S. Smith, A. Tumanov, E. W. Varnes

Princeton University, Princeton, NJ 08544, USA

G. Cavoto, D. del Re, R. Faccini,[5] F. Ferrarotto, F. Ferroni, E. Lamanna, E. Leonardi, M. A. Mazzoni, S. Morganti, G. Piredda, F. Safai Tehrani, M. Serra, C. Voena

Università di Roma La Sapienza, Dipartimento di Fisica and INFN, I-00185 Roma, Italy

S. Christ, R. Waldi

Universität Rostock, D-18051 Rostock, Germany

T. Adye, B. Franek, N. I. Geddes, G. P. Gopal, S. M. Xella

Rutherford Appleton Laboratory, Chilton, Didcot, Oxon, OX11 0QX, United Kingdom

N. Copty, M. V. Purohit, H. Singh, F. X. Yumiceva

University of South Carolina, Columbia, SC 29208, USA

I. Adam, P. L. Anthony, D. Aston, K. Baird, N. Berger, E. Bloom, A. M. Boyarski, F. Bulos, G. Calderini, M. R. Convery, D. P. Coupal, D. H. Coward, J. Dorfan, W. Dunwoodie, R. C. Field, T. Glanzman, G. L. Godfrey, S. J. Gowdy, P. Grosso, T. Haas, T. Himel, T. Hryn'ova, M. E. Huffer, W. R. Innes, C. P. Jessop, M. H. Kelsey, P. Kim, M. L. Kocian, U. Langenegger, D. W. G. S. Leith, S. Luitz, V. Luth, H. L. Lynch, H. Marsiske, S. Menke, R. Messner, K. C. Moffeit, R. Mount, D. R. Muller, C. P. O'Grady, V. E. Ozcan, M. Perl, S. Petrak, H. Quinn, B. N. Ratcliff, S. H. Robertson, L. S. Rochester, A. Roodman, T. Schietinger, R. H. Schindler, J. Schwiening, V. V. Serbo, A. Snyder, A. Soha, S. M. Spanier, J. Stelzer, D. Su, M. K. Sullivan, H. A. Tanaka, J. Va'vra, S. R. Wagner, A. J. R. Weinstein, W. J. Wisniewski, D. H. Wright, C. C. Young

Stanford Linear Accelerator Center, Stanford, CA 94309, USA

P. R. Burchat, C. H. Cheng, D. Kirkby, T. I. Meyer, C. Roat

Stanford University, Stanford, CA 94305-4060, USA

R. Henderson

TRIUMF, Vancouver, BC, Canada V6T 2A3

W. Bugg, H. Cohn, A. W. Weidemann

University of Tennessee, Knoxville, TN 37996, USA

[5] Also with University of California at San Diego, La Jolla, CA 92093, USA

J. M. Izen, I. Kitayama, X. C. Lou
University of Texas at Dallas, Richardson, TX 75083, USA

F. Bianchi, M. Bona, D. Gamba, A. Smol
Università di Torino, Dipartimento di Fiscia Sperimentale and INFN, I-10125 Torino, Italy

L. Bosisio, G. Della Ricca, L. Lanceri, P. Poropat, G. Vuagnin
Università di Trieste, Dipartimento di Fisica and INFN, I-34127 Trieste, Italy

R. S. Panvini
Vanderbilt University, Nashville, TN 37235, USA

C. M. Brown, P. D. Jackson, R. Kowalewski, J. M. Roney
University of Victoria, Victoria, BC, Canada V8W 3P6

H. R. Band, E. Charles, S. Dasu, F. Di Lodovico, A. M. Eichenbaum, H. Hu, J. R. Johnson, R. Liu, Y. Pan, R. Prepost, I. J. Scott, S. J. Sekula, J. H. von Wimmersperg-Toeller, S. L. Wu, Z. Yu
University of Wisconsin, Madison, WI 53706, USA

T. M. B. Kordich, H. Neal
Yale University, New Haven, CT 06511, USA

1 Introduction

One of the most important goals of the *BABAR* experiment is to precisely measure the angles of the Unitarity Triangle. While the decay $B^0 \to J/\psi K^0_S$ can be used to measure sin2β, the Standard Model predicts that the time-dependent *CP*-violating asymmetries in the decays $B^0 \to D^{(*)+}D^{(*)-}$ can also be used to measure the same quantity [1]. An independent measurement of sin2β in $B^0 \to D^{(*)+}D^{(*)-}$ modes is especially important since several typical extensions to the Standard Model can lead to different assymmetries between this quantity in $B^0 \to D^{(*)+}D^{(*)-}$ events and charmonium events [2]. Measurements of sin2β in $B^0 \to D^{(*)+}D^{(*)-}$ would thus provide stringent tests of *CP*-violation in the Standard Model and have significant potential to indicate deviations from it. However, the vector-vector decay $B^0 \to D^{*+}D^{*-}$ is not a pure *CP* eigenstate and a sizeable dilution of the measured asymmetry can be produced by a non-negligible *P*-wave *CP*-odd component. The dilution can, in principle, be completely removed by a time-dependent angular analysis of the decay products [3].

The rate for the Cabibbo-suppressed decays $B \to D^{(*)}\overline{D}^{(*)}$ can be estimated from the measured rate of the Cabibbo-favored decays $B \to D_s^{(*)}\overline{D}^{(*)}$:

$$\mathcal{B}(B \to D^{(*)}\overline{D}^{(*)}) \approx \left(\frac{f_{D^{(*)}}}{f_{D_s^{(*)}}}\right) \tan^2\theta_C \cdot \mathcal{B}(B \to D_s^{(*)}\overline{D}^{(*)}), \quad (1)$$

where θ_C is the Cabibbo angle, and $f_{D^{(*)}}$ and $f_{D_S^{(*)}}$ are decay constants. From this it follows that the $B \to D^{(*)}\overline{D}^{(*)}$ branching fractions are of the order of 10^{-3}. Previous measurements of branching fractions and upper limits for these modes are summarized in Table 1.

In section 2 we describe briefly the *BABAR* detector and the dataset. Section 3 describes the measurement of the branching fraction $B^0 \to D^{*+}D^{*-}$ and section 4 the corresponding angular analysis to extract the CP-even component of the decay. Finally, in section 5 we discuss the observation of the decays $B^0 \to D^{*+}D^-$ and $B^+ \to D^{*+}D^{*0}$. Section 6 summarizes our results.

Table 1: Summary of branching fraction and upper limit measurements performed by the CLEO [4] and ALEPH [5] experiments. Upper limits are quoted at the 90% confidence level.

Decay		Branching Fraction ($\times 10^{-4}$)
$B^0 \to D^{*+}D^{*-}$	[4]	$9.9^{+4.2}_{-3.3}(stat) \pm 1.2(syst)$
$B^0 \to D^{*+}D^-$	[4]	< 6.3
$B^+ \to D^{*+}D^{*0}$	[5]	$< 110.$

2 The *BABAR* detector and dataset

The data used in this analysis were collected with the *BABAR* detector [6] at the PEP-II storage ring [7] located at the Stanford Linear Accelerator Center. This data sample represents an integrated luminosity of 23.3 fb^{-1}, with 20.7 fb^{-1} collected on the $\Upsilon(4S)$ resonance. The total number of $B\overline{B}$ pairs produced in this sample was $N_{B\overline{B}} = (22.7 \pm 0.36) \times 10^6$.

Charged particles are detected and their momenta measured with the combination of a 40-layer drift chamber (DCH) and a five-layer silicon vertex tracker (SVT) embedded in a 1.5 T solenoidal

magnetic field. Photons are detected by a CsI electromagnetic calorimeter (EMC) that provides excellent angular and energy resolutions with a high efficiency for energies above 20 MeV. Charged particle identification is provided by the specific ionization loss ($\mathrm{d}E/\mathrm{d}x$) in the tracking devices and by an internally reflecting ring-imaging Cherenkov detector (DIRC) covering the barrel region of the detector.

3 Measurement of the $B^0 \to D^{*+}D^{*-}$ branching Fraction

B^0 mesons are exclusively reconstructed by combining two charged D^* candidates reconstructed in a number of D^* and D decay modes. Events are pre-selected by requiring that there be three or more charged tracks and that the normalized second Fox-Wolfram moment [8] of the event be less than 0.6. We also require that the cosine of the angle between the reconstructed B direction and the thrust axis of the rest of the event be less than 0.9.

Charged kaon candidates are required to be inconsistent with the pion hypothesis, as inferred from the Cherenkov angle measured by the DIRC and the specific ionization measured by the SVT and DCH. No particle identification requirements are made for the kaon from the decay $D^0 \to K^-\pi^+$.

$K^0_S \to \pi^+\pi^-$ candidates are required to have an invariant mass within $25\,\mathrm{MeV}/c^2$ of the nominal K^0_S mass [9]. The opening angle between the flight direction and the momentum vector of the K^0_S candidate is required to be less than 200 mrad, and the transverse flight distance from the primary event vertex must be greater than 2 mm.

Neutral pion candidates are formed from pairs of photons in the EMC with energy above 30 MeV, an invariant mass within $20\,\mathrm{MeV}/c^2$ of the nominal π^0 mass, and a summed energy greater than 200 MeV. A mass-constraint fit is then applied to these π^0 candidates. The π^0 from $D^{*+} \to D^+\pi^0$ decays ("soft" π^0), however, is required to have an invariant mass within $35\,\mathrm{MeV}/c^2$ of the nominal π^0 mass and momentum in the $\Upsilon(4S)$ frame of $70 < p^* < 450\,\mathrm{MeV}/c$, with no requirement on the summed photon energies.

The decay modes of the D^0 and D^+ used in this analysis were selected by an optimization of $S^2/(S+B)$ based on Monte Carlo simulations, where S is the expected number of signal events and B is the expected number of background events. The D^0 and D^+ modes used and their branching fractions are summarized in Table 2. D^0 (D^+) meson candidates are required to have an invariant mass within $20\,\mathrm{MeV}/c^2$ of the nominal D^0 (D^+) mass.

The D^{*+} mesons are reconstructed in their decays $D^{*+} \to D^0\pi^+$ and $D^{*+} \to D^+\pi^0$. We include for this analysis the decay combinations $D^{*+}D^{*-}$decaying to ($D^0\pi^+$, $D^0\pi^-$) or ($D^0\pi^+$, $D^-\pi^0$), but not ($D^+\pi^0$,$D^-\pi^0$) due to the smaller branching fraction and larger expected backgrounds. The branching fractions for these modes are summarized in Table 3. D^0 and D^+ candidates are subjected to a mass-constraint fit and then combined with soft pion candidates. A vertex fit is performed that includes the position of the beam spot to improve the angular resolution of the soft pion.

To select B^0 candidates with well reconstructed D^* and D mesons, we construct a χ^2 that includes all measured D^* and D masses:

$$\chi^2_{Mass} = \left(\frac{m_D - m_{D_{PDG}}}{\sigma_{m_D}}\right)^2 + \left(\frac{m_{\overline{D}} - m_{\overline{D}_{PDG}}}{\sigma_{m_{\overline{D}}}}\right)^2 + \left(\frac{\Delta m_{D^*} - \Delta m_{D^*_{PDG}}}{\sigma_{\Delta m_{D^*}}}\right)^2 + \left(\frac{\Delta m_{\overline{D}^*} - \Delta m_{D^*_{PDG}}}{\sigma_{\Delta m_{D^*}}}\right)^2$$

Table 2: D^0 and D^+ decay modes and branching fractions [9]. The branching fraction for $K^0_S \to \pi^+\pi^-$ is included for modes containing a K^0_S.

Decay Mode	Branching Fraction (%)
$D^0 \to K^-\pi^+$	3.83 ± 0.09
$D^0 \to K^-\pi^+\pi^0$	13.9 ± 0.9
$D^0 \to K^-\pi^+\pi^+\pi^-$	7.49 ± 0.31
$D^0 \to K^0_S\pi^+\pi^-$	1.85 ± 0.14
Total D^0 Branching Fraction	27.1
Decay Mode	Branching Fraction (%)
$D^+ \to K^-\pi^+\pi^+$	9.0 ± 0.6
$D^+ \to K^0_S\pi^+$	0.99 ± 0.09
$D^+ \to K^-K^+\pi^+$	0.87 ± 0.07
Total D^+ Branching Fraction	10.9

Table 3: D^* and D^{*0} decay modes and branching fractions [9]. D^{*0} is used for the $B^+ \to D^{*+}D^{*0}$ analysis described in Section 5.

Particle	Decay Mode	Branching Fraction (%)
D^{*+}	$D^{*+} \to D^0\pi^+$	67.7 ± 0.5
	$D^{*+} \to D^+\pi^0$	30.7 ± 0.5
Total Visible D^{*+} Branching Fraction		98.4
D^{*0}	$D^{*0} \to D^0\pi^0$	61.9 ± 2.9
	$D^{*0} \to D^0\gamma$	38.1 ± 2.9
Total D^{*0} Branching Fraction		100.0

where the subscript PDG refers to the nominal value, and Δm_{D^*} is the $D^* - D$ mass difference. For σ_{m_D} we use values computed for each D candidate, while for $\sigma_{\Delta m_{D^*}}$ we use fixed values of $0.83\,\mathrm{MeV}/c^2$ for $D^{*+} \to D^0\pi^+$ and $1.18\,\mathrm{MeV}/c^2$ for $D^{*+} \to D^+\pi^0$. A requirement that $\chi^2_{Mass} < 20$ is applied to all B^0 candidates. In events with more than one B^0 candidate, we choose the candidate with the lowest value of χ^2_{Mass}.

A B meson candidate is characterized by two kinematic variables. We use the energy-substituted mass, $m_{\rm ES}$, defined as

$$m_{\rm ES} \equiv \sqrt{E^{*2}_{Beam} - {p^*_B}^2}$$

and the difference of the B candidate's energy from the beam energy, ΔE ,

$$\Delta E \equiv E^*_B - E^*_{Beam}$$

where E^*_B (p^*_B) are the energy (momentum) of the B candidate in the center-of-mass frame and E^*_{Beam} is one-half of the center-of-mass energy. The signal region in the ΔE *vs.* $m_{\rm ES}$ plane is defined to be $|\Delta E| < 25\,\mathrm{MeV}$ and $5.273 < m_{\rm ES} < 5.285\,\mathrm{GeV}/c^2$. The width of this region corresponds to approximately $\pm 2.5\sigma$ in both ΔE and $m_{\rm ES}$.

These values on χ^2_{Mass}, $m_{\rm ES}$, and ΔE were chosen based on an optimization of $S^2/(S+B)$, where S is the expected number of signal events and B is the expected number of background events. The optimization process was done entirely with samples of signal and generic $B\overline{B}$ and $c\overline{c}$ Monte Carlo where the background distribution is taken from a sideband region, defined as

$$|\Delta E| < 200\,{\rm MeV}$$

$$5.20\,{\rm GeV}/c^2 < m_{\rm ES} < 5.26\,{\rm GeV}/c^2$$

and

$$50\,{\rm MeV} < |\Delta E| < 200\,{\rm MeV}$$

$$5.26 < m_{\rm ES} < 5.29\,{\rm GeV}/c^2$$

These values were chosen based on a maximization of $S^2/(S+B)$ with a tendency towards looser cut values to reduce any possible systematic error incurred due to the differences in the reconstructed mass resolutions between data and Monte Carlo.

To determine the number of signal events in the signal region, we must estimate the expected contribution from background. This is done by scaling the number of events seen in the data sideband (defined above) with a scaling factor which gives a measure of the relative areas of the signal region to the sideband region. We parameterize the shape of the background in the ΔE *vs.* $m_{\rm ES}$ plane as the product of an ARGUS function [10] in $m_{\rm ES}$ and a first-order polynomial in ΔE . Based on this parameterization we estimate that the ratio of the number of background events in the signal region to the number in the sideband region is $(1.72 \pm 0.10) \times 10^{-2}$. The uncertainty is derived from the observed variation of this ratio under alternative assumptions for the background shape in $m_{\rm ES}$ and ΔE .

Figure 1 shows the events in the ΔE *vs.* $m_{\rm ES}$ plane after all selection criteria have been applied. The small box in the figure indicates the signal region defined above, and the sideband is the entire plane excluding the region bounded by the larger box outside the signal region. There are a total of 38 events located in the signal region, with 363 events in the sideband region. The latter, together with the effective ratio of areas of the signal region to the sideband region, implies an expected number of background events in the signal region of $6.24 \pm 0.33(stat) \pm 0.36(syst)$. The quoted systematic uncertainty comes from the background shape variation discussed previously. Figure 2 shows a projection of the data on the $m_{\rm ES}$ axis after requiring $|\Delta E| < 25\,{\rm MeV}$.

We use a detailed Monte Carlo simulation of the *BABAR* detector to determine the efficiency for reconstructing the signal. This, together with the total number of $B\overline{B}$ pairs produced during data collection, allows us to determine a preliminary branching fraction for $B^0 \to D^{*+}D^{*-}$ to be

$$\mathcal{B}(B^0 \to D^{*+}D^{*-}) = (8.0 \pm 1.6(stat) \pm 1.2(syst)) \times 10^{-4}$$

The dominant systematic uncertainty in this measurement comes from our level of understanding of the charged particle tracking efficiency (9.4%). The high charged particle multiplicity in this decay mode makes this measurement particularly sensitive to tracking efficiency. Systematic errors were assigned on a per track basis for π, K and slow π, and were added linearly due to large correlations. The imprecisely known partial-wave content of the $B^0 \to D^{*+}D^{*-}$ final state is another source of systematic biases. Monte Carlo events in each of the two extremes of transversity amplitudes $(A_{//}, \sqrt{2}A_0, A_\perp) = (1., 0., 0.)$ and $(0., 1., 0.)$ were generated and reconstructed [11]. Although both mixtures correspond to $R_t = 0$, the resulting p_t distributions of the slow pion represent the two extreme cases of possible p_t distributions. The change in the reconstruction efficiency of these

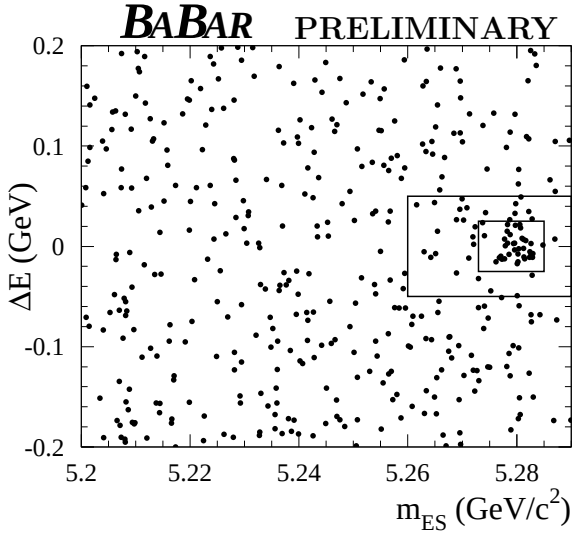

Figure 1: Distribution of $B^0 \to D^{*+}D^{*-}$ events in the ΔE *vs.* $m_{\rm ES}$ plane. The small box indicates the signal region, while the sideband region is everything outside the larger box.

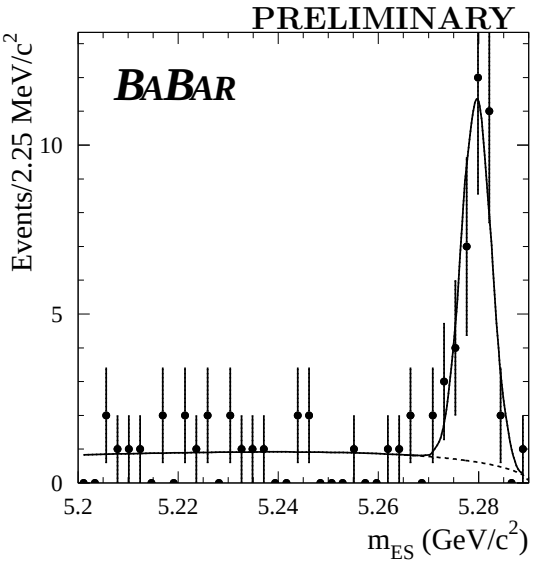

Figure 2: Distribution of $B^0 \to D^{*+}D^{*-}$ events in $m_{\rm ES}$ plane with a cut of $|\Delta E| < 25$ MeV applied. The curve represents a fit to the distribution of the sum of a Gaussian to model the signal and an ARGUS function [10] to model the background shape.

final angular states is quoted as systematic error (6.6%). Other significant systematic biases arise due to the uncertainties on the D^{*+}, D^0 and D^+ branching fractions (5.6%) and the differences in mass resolutions between Monte Carlo and data (4.1%). Possible contributions from peaking backgrounds was found to be negligable.The total systematic uncertainty from all sources is 14.5%.

4 Determination of the CP content of $B^0 \to D^{*+}D^{*-}$

The fraction of the CP-odd component, R_t, of the decay $B^0 \to D^{*+}D^{*-}$ can be determined from the angular distribution in the transversity basis [3]:

$$\frac{1}{\Gamma}\frac{\mathrm{d}\Gamma}{\mathrm{d}\cos\theta_{\mathrm{tr}}} = \frac{3}{4}(1-R_t)\sin^2\theta_{tr} + \frac{3}{2}R_t\cos^2\theta_{tr} \tag{2}$$

Here Γ is the decay rate and θ_{tr} is the polar angle defined as the angle between the normal to the D^{*-} decay plane and the π^+ line of flight in the D^{*+} rest frame.

We perform an unbinned maximum likelihood fit to the 38 events in the signal region described in the previous section. The fit takes into account the presence of background, whose properties are derived from the sideband sample, and the angular resolution $\sigma_{\theta_{tr}}$ estimated from the simulated data samples. We define the likelihood function to be

$$\begin{aligned}\mathcal{L} = \prod_{i=1,n}\mathcal{L}_i = \prod_{i=1,n}\Big[&p\times\mathcal{F}(\theta_{tr,i},\sigma_{\theta,i},R_t^{sig})+\\ &(1-p)\times\mathcal{F}(\theta_{tr,i},\sigma_{\theta,i},R_t^{bkg})\Big],\end{aligned} \tag{3}$$

where n is the number of selected events and the contribution to the total likelihood from the i-th event, $\mathcal{L}_i$, is defined in terms of the purity p of the sample and the probability density functions $\mathcal{F}(\theta_{tr,i},\sigma_{\theta,i},R_t)$ for the signal and background: R_t^{sig} and R_t^{bkg} are the parameters describing the shapes of the signal and background angular distributions, respectively, and $\theta_{tr,i}$ is the measured transversity angle in event i. The probability density functions $\mathcal{F}$ are obtained from the convolution of the angular distribution (Eq. 2) with Gaussian resolution functions describing the measurement errors $\sigma_{\theta,i}$. We note that Eq. 2 is the differential decay rate Γ integrated over the full ranges of the other two decay angles in the transversity basis; this assumes a flat acceptance and needs to be corrected for in the final determination of R_t. An empirical study of the events in the sideband region showed that the background angular distribution can be described as constant in $\cos\theta_{tr}$, as expected. The parameterization in Eq. 3 can describe deviations from this behaviour and was used to estimate the background contribution to the systematic uncertainty on R_t.

The fit procedure was tested on several samples of $B^0 \to D^{*+}D^{*-}$ Monte Carlo events generated with different R_t values and different sets of decay amplitudes in order to determine the possible bias induced by angular acceptance effects correlated with the inefficiency in detecting soft pions from D^* decays below a threshold in transverse momentum of about 70 MeV/c. The fitted R_t values were fully consistent with the generated values in the limit of negligible soft pion inefficiency, but could be biased, depending on the decay amplitudes, when the pion detection threshold was taken into account. A correction and a systematic error were estimated to describe these effects (described below).

The value of R_t^{bkg} was evaluated by fitting the 363 events in the sideband region and setting $p = 0$ in Eq. 3. The result of this fit was $R_t^{bkg} = 0.29 \pm 0.04$, compatible with the value expected for a flat distribution ($R_t = 1/3$).

To determine R_t^{sig}, we fit the 38 events in the signal region with R_t^{bkg} fixed to 0.29 and p fixed at 83.6%. The result of the fit to the signal region, without correction for angular acceptance bias, is $R_t^{sig} = 0.25 \pm 0.18(stat)$, and is shown in Figure 3. The fit was repeated with both R_t^{sig} and R_t^{bkg} floating, giving the same central values with a rather small correlation (-0.04) between the parameters.

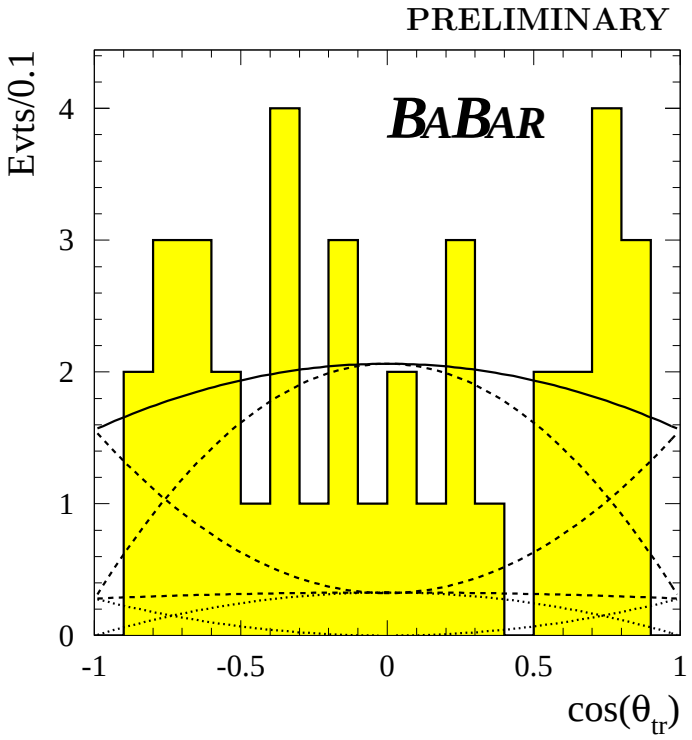

Figure 3: The $\cos\theta_{tr}$ distribution from the unbinned ML fit, superimposed on the histogram of the $B^0 \to D^{*+}D^{*-}$ candidates in the signal region. The dotted and dashed lines represent the fitted *CP* components for the signal and background contributions. The lower two dotted curves represent the two background fitted components, proportional to $\sin^2\theta_{tr}$ and $\cos^2\theta_{tr}$ respectively; their sum (dashed curve) is almost constant at about 0.3 events/bin. Similarly, the two upper dashed curves represent the *CP* components of the signal. The solid line represents the $\cos\theta_{tr}$ distribution from the unbinned ML fit for the selected events.

The dominant systematic uncertainty on the measured value of R_t comes from the acceptance bias due to the transverse momentum threshold in the detection of soft pions. This bias ranges between -0.048 and $+0.004$, and depends on the yet unknown decay amplitudes. The central value of this interval was taken as a correction to the fitted R_t^{sig}, while its half width was assumed as a contribution to the systematic error. Other contributions come from the imperfect knowledge of the finite resolution on the measured value of θ_{tr} (0.006), of the angular distribution of the background (0.008) and of the purity of the signal sample (0.0003). All uncertainties were evaluated with Monte Carlo simulations. The total systematic uncertainty on R_t was determined to be 0.031, giving the final corrected result:

$$R_t = 0.22 \pm 0.18(stat) \pm 0.03(syst)$$

The likelihood function was also used to estimate approximate confidence intervals, taking into account the allowed physical region. Fig. 4 shows the dependence of $L_{data}(R_t) = -2\ln(\mathcal{L}(R_t)/\mathcal{L}(\bar{R}_t))$ on R_t, where $\bar{R}_t$ is the value of R_t that maximizes $\mathcal{L}(R_t)$. The lines corresponding to the 68%, 95%, 99% confidence level limits on R_t are also plotted. We can exclude values of R_t greater than 0.63 at the 95% confidence level.

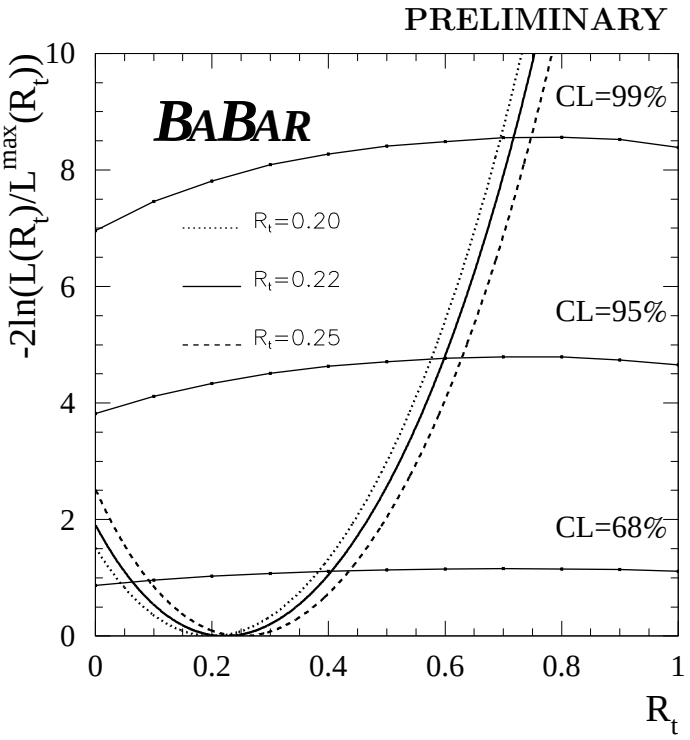

Figure 4: Likelihood ratio $L_{data}(R_t) = -2\ln(\mathcal{L}(R_t)/\mathcal{L}(\bar{R}_t))$ for the data, where $\bar{R}_t$ is the value of R_t that maximizes $\mathcal{L}(R_t)$, and 68%, 95%, 99% confidence level limits on R_t. The systematic error on R_t is indicated by the dotted and dashed lines.

5 Observation of the decays $B^0 \to D^{*+}D^-$ and $B^+ \to D^{*+}D^{*0}$

The decays $B^0 \to D^{*+}D^-$ and $B^+ \to D^{*+}D^{*0}$ are studied following a method largely similar to that described in Sec. 3. Here, only those aspects of the analyses that differ significantly from that of the $B^0 \to D^{*+}D^{*-}$ analysis are discussed in some detail.

For $B^0 \to D^{*+}D^-$, B^0 mesons are exclusively reconstructed by combining a $D^{*\pm}$ and a $D^{\mp}$ candidate that are reconstructed in a number of $D^{*\pm}$ and $D^{\mp}$ decay modes. For $B^+ \to D^{*+}D^{*0}$ the exclusive reconstruction combines a $D^{*\pm}$ and a D^{*0}. The kaon flavor of the D^{*0} is checked to make sure that a D^{*+} is paired only with a $\overline{D}^{*0}$ and a D^{*-} is only paired with a D^{*0}. The selection of $D^{\pm}$ and $D^{*\pm}$ candidates, and the K^0_S and π^0 candidates that are used to compose them, is identical to that described for the $B^0 \to D^{*+}D^{*-}$ analysis.

The decay modes of the D and D^* used in these analyses are selected by an optimization of $S^2/(S+B)$ based on Monte Carlo simulations. $D^{*\pm}$ mesons are reconstructed in their decays $D^{*+} \to D^0\pi^+$ and $D^{*+} \to D^+\pi^0$, and D^{*0} mesons are reconstructed in their decays $D^{*0} \to D^0\pi^0$ and $D^{*0} \to D^0\gamma$. Modes used and their branching fractions are summarized in Tables 2 and 3. As in the $B^0 \to D^{*+}D^{*-}$ analysis, we construct χ^2_{Mass} variables that include all measured $D^{*\pm}$, D^{*0}, and D masses. For $B^+ \to D^{*+}D^{*0}$, χ^2_{Mass} contains 4 terms:

$$\chi^2_{Mass} = \left(\frac{m_D - m_{D_{PDG}}}{\sigma_{m_D}}\right)^2 + \left(\frac{m_{\overline{D}} - m_{\overline{D}_{PDG}}}{\sigma_{m_{\overline{D}}}}\right)^2 + \left(\frac{\Delta m_{D^*} - \Delta m_{D^*_{PDG}}}{\sigma_{\Delta m_{D^*}}}\right)^2 + \left(\frac{\Delta m_{D^{*0}} - \Delta m_{D^{*0}_{PDG}}}{\sigma_{\Delta m_{D^{*0}}}}\right)^2$$

For $B^0 \to D^{*+}D^-$, χ^2_{Mass} contains 3 terms:

$$\chi^2_{Mass} = \left(\frac{m_D - m_{D_{PDG}}}{\sigma_{m_D}}\right)^2 + \left(\frac{m_{D_{D^*}} - m_{D_{PDG}}}{\sigma_{m_{D_{D^*}}}}\right)^2 + \left(\frac{\Delta m_{D^*} - \Delta m_{D^*_{PDG}}}{\sigma_{\Delta m_{D^*}}}\right)^2$$

The major difference between these analyses and the $B^0 \to D^{*+}D^{*-}$ analysis is that the χ^2_{Mass} cut values for these analyses are set individually for each submode instead of having a global χ^2_{Mass} value for all submodes, to better take into account the fact that the amount of background is quite different for each of the different submodes in these analyses. The procedure used to optimize the χ^2_{Mass} value chooses the individual values of χ^2_{Mass} that together maximize the global $S^2/(S+B)$. Submodes which have an optimal value of less than 2 times the number of degrees of freedom of the χ^2_{Mass} (8 for $B^+ \to D^{*+}D^{*0}$, 6 for $B^0 \to D^{*+}D^-$) are rejected on the grounds that the resulting sensitivity is poor, and that the tightness of the χ^2_{Mass} value makes such modes more susceptible to systematic errors in measured yield.

These values were tuned with samples of signal and generic $B\overline{B}$ and $c\overline{c}$ Monte Carlo where the background distribution is taken from a sideband region. For $B^+ \to D^{*+}D^{*0}$, the sideband region is the same as that for $B^0 \to D^{*+}D^{*-}$. For $B^0 \to D^{*+}D^-$, the region where decays (such as $B^0 \to D^{*+}D^{*-}$) can feed down into the ΔE -$m_{\rm ES}$ plane must be eliminated from the sideband. As $B^0 \to D^{*+}D^{*-}$ contains a reconstructed $D^{*\pm}$ and D, it is only separated from $B^0 \to D^{*+}D^-$ events due to the missing energy of the slow pion from the second $D^{*\pm}$. This missing energy manifests itelf as a negative shift in ΔE . These events accumulate in the area below the $B^0 \to D^{*+}D^-$ signal region, and in order to remove them, the region defined by:

$$\Delta E < -50\,\mathrm{MeV}$$

$$m_{\rm ES} > 5.26\,\mathrm{GeV}/c^2$$

is removed. The $m_{\rm ES}$ and ΔE distributions for events reconstructed in the channels $B^0 \to D^{*+}D^-$ and $B^+ \to D^{*+}D^{*0}$ are shown in Fig. 5 and in Fig. 6.

For the $B^0 \to D^{*+}D^-$ channel we reconstruct a total of 31 events, of which $10.5 \pm 1.7(stat)$ are background. The probability that the visible signal is a statistical fluctuation of the background is 9.7×10^{-7} ($> 4.3\sigma$). As pointed out in the introduction, this channel is a *CP* conjugate state that can be used for sin2β measurements. For $B^+ \to D^{*+}D^{*0}$ we reconstruct a total of 39 events, of which $20.3 \pm 0.5(stat)$ are background. The probability that the visible signal is a statistical fluctuation of the background is 2.9×10^{-6} ($> 4.1\sigma$). This channel is useful for calibrations and tests of the *CP* fitting procedures.

6 Summary

Using data collected by the *BABAR* experiment during 1999-2000, we have observed a signal of $31.8 \pm 6.2(stat) \pm 0.4(syst)$ events in the decay $B^0 \to D^{*+}D^{*-}$. Our measurement of the branching

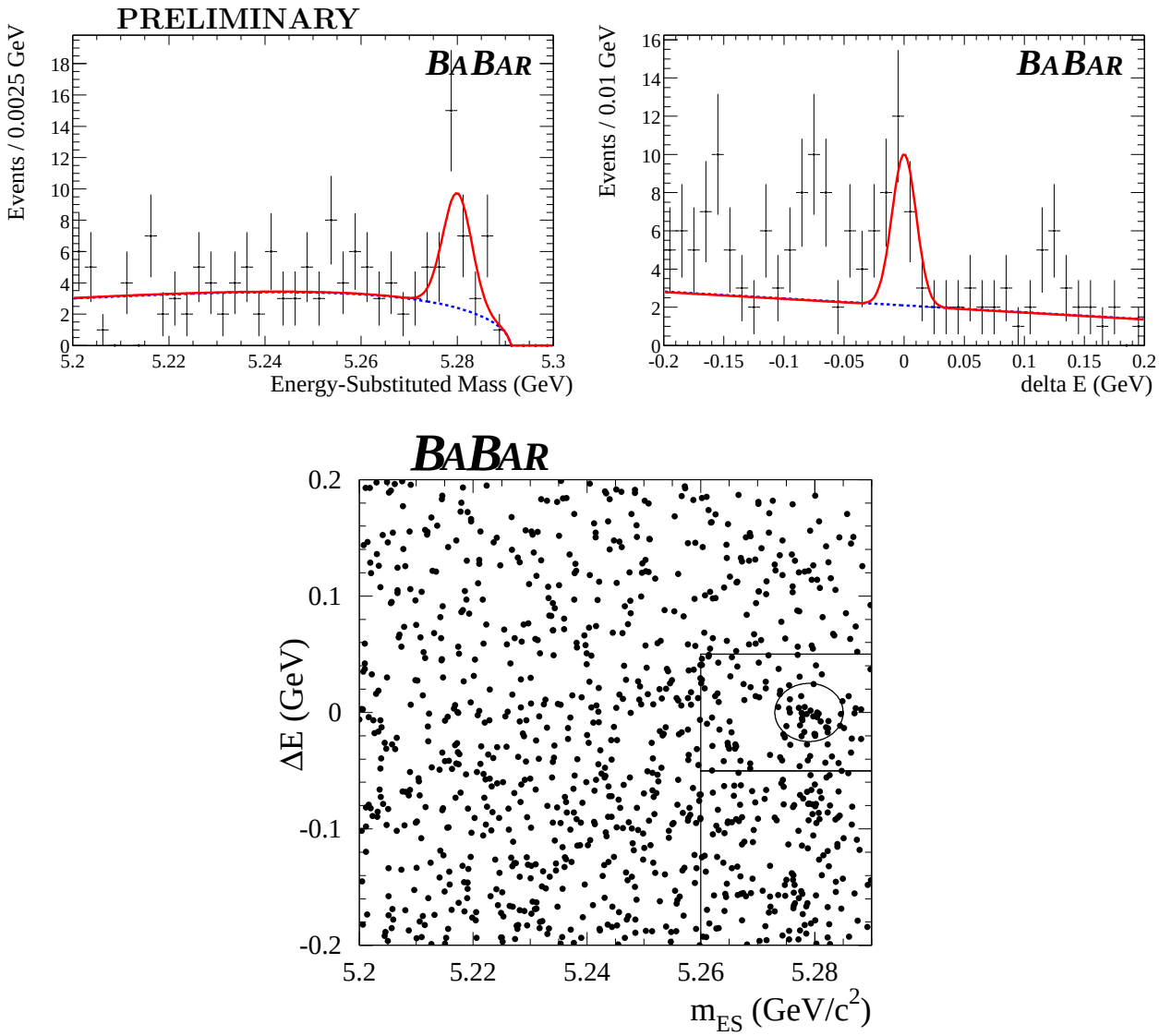

Figure 5: Top Left: $m_{\rm ES}$ projection of the $B^0 \to D^{*+}D^-$ event population, in the ΔE signal band ($-0.025 < \Delta E < 0.025\,{\rm GeV}$). The crosses are the data. The dashed line represents the extrapolation, to the ΔE signal band, of a two-dimensional background fit in the ΔE -$m_{\rm ES}$ sidebands. The solid line is the sum of this background extrapolation and of a fitted, Gaussian-shaped signal centered on the B mass. Top Right: ΔE projection of the $B^0 \to D^{*+}D^-$ event population, in the $m_{\rm ES}$ signal band ($5.273 < m_{\rm ES} < 5.285\,{\rm GeV}/c^2$). The crosses are the data. The dashed line represents the extrapolation, to the $m_{\rm ES}$ signal band, of the above-mentioned background fit. The solid line is the sum of this background extrapolation, and of a gaussian-shaped signal centered on $\Delta E = 0$. In the case of both the upper plots, the points in the feed-down region ($\Delta E < -0.05\,{\rm GeV}$) are excluded from the fits. Bottom: Two-dimensional distribution of the $B^0 \to D^{*+}D^-$ events in the ΔE *vs.* $m_{\rm ES}$ plane. The small ellipse indicates the signal region, while the sideband region is everything that is outside the box that surrounds the signal region and also outside the (feed-down) box below the signal region.

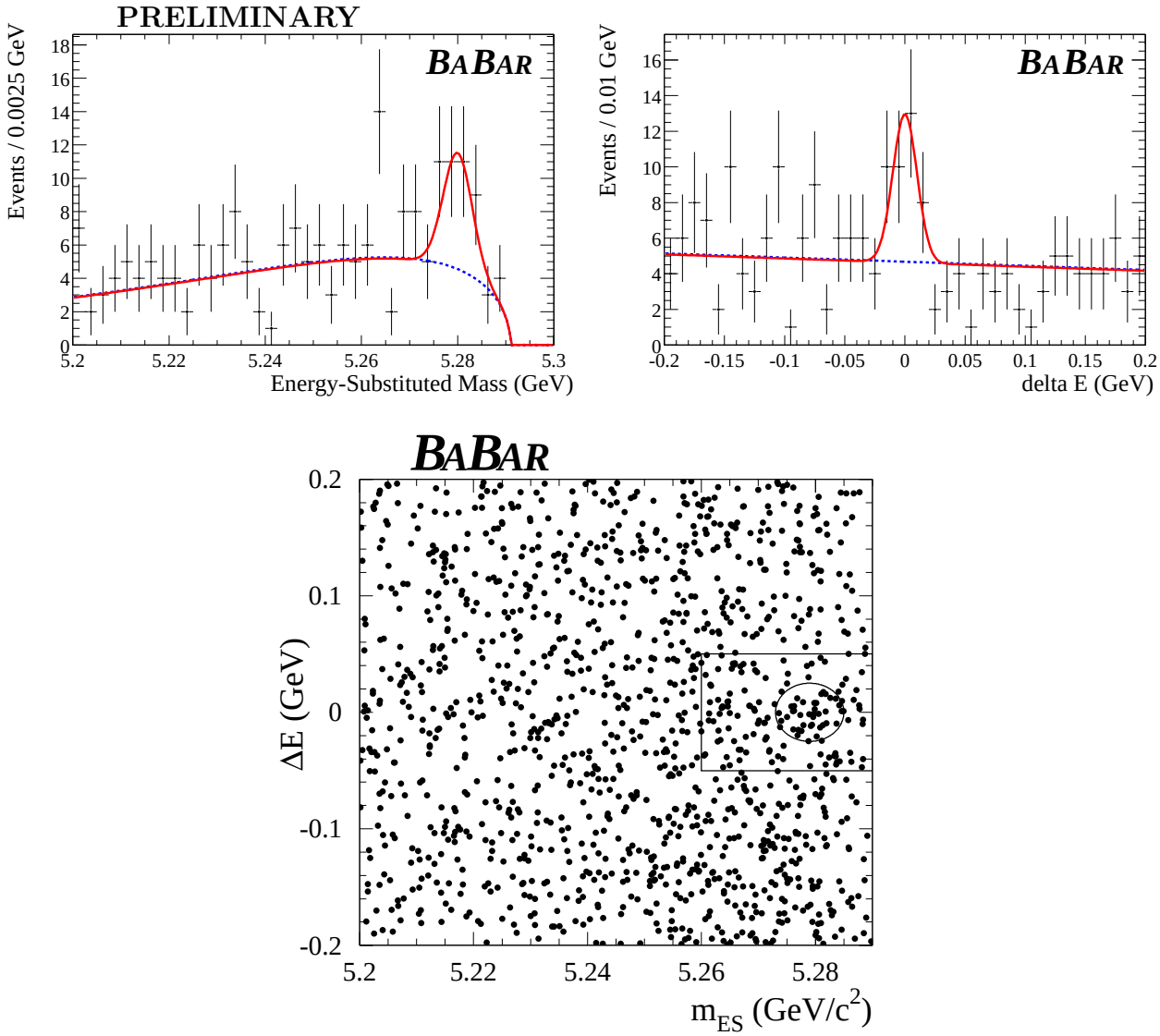

Figure 6: Top Left: $m_{\rm ES}$ projection of the $B^+ \to D^{*+}D^{*0}$ event population, in the ΔE signal band ($-0.025 < \Delta E < 0.025\,{\rm GeV}$). The crosses are the data. The dashed line represents the extrapolation, to the ΔE signal band, of a two-dimensional background fit in the ΔE -$m_{\rm ES}$ sidebands. The solid line is the sum of this background extrapolation and of a fitted, Gaussian-shaped signal centered on the B mass. Top Right: ΔE projection of the $B^+ \to D^{*+}D^{*0}$ event population, in the $m_{\rm ES}$ signal band ($5.273 < m_{\rm ES} < 5.285\,{\rm GeV}/c^2$). The crosses are the data. The dashed line represents the extrapolation, to the $m_{\rm ES}$ signal band, of the above-mentioned background fit. The solid line is the sum of this background extrapolation, and of a Gaussian-shaped signal centered on $\Delta E = 0$. Bottom: Two-dimensional distribution of the $B^+ \to D^{*+}D^{*0}$ events in the ΔE *vs.* $m_{\rm ES}$ plane. The small ellipse indicates the signal region, while the sideband region is everything that is outside the box that surrounds the signal region.

ratio is

$$\mathcal{B}(B^0 \to D^{*+}D^{*-}) = (8.0 \pm 1.6(stat) \pm 1.2(syst)) \times 10^{-4}$$

From the transversity angular distribution of these events, the measured fraction of the component with odd *CP* parity is

$$R_t = 0.22 \pm 0.18(stat) \pm 0.03(syst)$$

Finally, signals are also observed in the decay modes $B^0 \to D^{*+}D^-$ and $B^+ \to D^{*+}D^{*0}$.

7 Acknowledgments

We are grateful for the extraordinary contributions of our PEP-II colleagues in achieving the excellent luminosity and machine conditions that have made this work possible. The collaborating institutions wish to thank SLAC for its support and the kind hospitality extended to them. This work is supported by the US Department of Energy and National Science Foundation, the Natural Sciences and Engineering Research Council (Canada), Institute of High Energy Physics (China), the Commissariat à l'Energie Atomique and Institut National de Physique Nucléaire et de Physique des Particules (France), the Bundesministerium für Bildung und Forschung (Germany), the Istituto Nazionale di Fisica Nucleare (Italy), the Research Council of Norway, the Ministry of Science and Technology of the Russian Federation, and the Particle Physics and Astronomy Research Council (United Kingdom). Individuals have received support from the Swiss National Science Foundation, the A. P. Sloan Foundation, the Research Corporation, and the Alexander von Humboldt Foundation.

References

[1] Charge-conjugate states are implied throughout this paper and the symbol $D^{(*)}$ refers to either D or D^*.

[2] Y. Grossman and M. Worah, Phys. Lett. B **395**, 241 (1997);
R. Fleischer, Int. Jour. Mod. Phys. **A 12**, 2459 (1997).

[3] I. Dunietz *et al.*, Phys. Rev. D **43**, 2193 (1991).

[4] E. Lipeles *et al.*, Phys. Rev. D **62**, 032005 (2000).

[5] R. Barate *et al.*, Eur. Phys. Jour. **C4**, 387 (1998).

[6] The *BABAR* Collaboration, B. Aubert *et al.*, SLAC-PUB-8596, hep-ex/0105044, to appear in Nucl. Instrum. Methods.

[7] PEP-II Conceptual Design Report, SLAC-R-418 (1993).

[8] G. C. Fox and S. Wolfram, Phys. Rev. Lett. **41**, 1581 (1978).

[9] Particle Data Group, D. E. Groom *et al.*, Eur. Phys. Jour. C **15**, 1 (2000).

[10] ARGUS Collaboration, H. Albrecht *et al.*, Phys. Lett. **B185**, 218 (1987).

[11] P. H. Harrison and H. R. Quinn, eds. "The *BABAR* Physics Book", SLAC-R-504 (1998).